www.ijecs.in
International Journal of Engineering and Computer Science
Volume 14 Issue 03 March 2025, Page No. 26982-26999
ISSN: 2319-7242 DOI: 10.18535/ijecs/v14i03.5034

Performance Evaluation of Interleaved Division Multiple Access Using Low Density Parity Check Forward Error Correcting Codes for 5G Wireless System

Hudu Burah [1], Samuel Ndueso John [2], Joshua Sokowonci Mommoh [3*], Etinosa NomaOsaghe [4], Solomon Iliya Zakwoi [1], Abubakar Bala [5]

[1] National Space Research and Development Agency, Nigeria
[2] Department of Electrical Electronic Engineering, Nigerian Defence Academy, Kaduna, 800281, Nigeria
[3] Department of Software Engineering, Mudiame University Irrua, Edo, 310112, Nigeria.
[4] Department of Electrical and Electronics Engineering, Olabisi Onabanjo University, Ogun, 120107, Nigeria.
[5] Department of Electrical and Electronics Engineering, Nigerian Army University, Biu, Borno, 603108, Nigeria.

Abstract
The increasing demand for high data rates, massive connectivity, and low latency in next-generation wireless communication systems could not be efficiently met using conventional orthogonal multiple access (OMA) schemes. This limitation necessitated the shift toward Non-Orthogonal Multiple Access (NOMA) techniques, particularly Interleaved Division Multiple Access (IDMA), which emerged as a promising candidate for 5G and beyond due to its improved system flexibility, spectral efficiency, and enhanced coverage. Despite these advantages, IDMA faced two critical challenges: optimal interleaver design and the selection of an efficient forward error correction (FEC) scheme. In this study, the performance of an LDPC-coded IDMA system employing a Gold sequence interleaver was analyzed under various conditions. The system's bit error rate (BER) performance was evaluated over Rayleigh fading and additive white Gaussian noise (AWGN) channels with different interleaving schemes and FEC techniques. The BER versus Eb/No (energy-per-bit-to-noise-power spectral density ratio) analysis revealed that the CDMA system exhibited a BER of 0.0026101, whereas the IDMA system achieved a significantly lower BER of 0.0004015, reflecting an 18.25% improvement in error performance. Moreover, the proposed Gold sequence interleaver, when integrated with LDPC, outperformed conventional interleavers, including random, convolutional, and tree interleavers, by attaining the lowest BER of 0.001312500 at 9 dB. These findings demonstrated that the Gold sequence-based LDPC-IDMA system achieved near-optimal performance while maintaining low computational complexity, making it suitable for practical 5G implementations.

Keywords: Interleaved Division Multiple Access (IDMA), Low-Density Parity-Check (LPDC), Gold Sequence Interleaver, Bit Error Rate (BER), Additive White Gaussian Noise (AWGN) and 5G Wireless Communication

1. Introduction

Over the last four decades, the evolution of wireless communication networks has significantly impacted various aspects of human life, including societal, political, cultural, and economic dimensions. The advancement of wireless communication systems, along with the rising demand for connectivity, has necessitated the expansion of multiple access (MA) strategies to optimize performance while efficiently utilizing available spectrum resources [1]. However, as

wireless communication applications continue to emerge and cellular networks become increasingly dense, unprecedented communication requirements must be satisfied to meet users' growing demands. These demands include increased coverage, high throughput, low latency, high efficiency, and low power consumption. A major transformation in communication networks has been the shift from orthogonal multiple access (OMA) to non-orthogonal multiple access (NOMA) technology, driven by the rapid evolution of technologies such as mobile Internet and the Internet of Things (IoT) [2], [3].

The evolution of wireless communication has seen various generations employing different MA techniques. 1G in the 1980s utilized Frequency Division Multiple Access (FDMA) with limited capacity. 2G 1990 introduced Time Division Multiple Access (TDMA) and Code Division Multiple Access (CDMA), enhancing capacity and security. 3G in the 2000s implemented Wideband CDMA (WCDMA), increasing data rates and multimedia capabilities. 4G 2010s adopted Orthogonal Frequency Division Multiple Access (OFDMA), offering higher spectral efficiency and reduced latency. All these generations relied on OMA schemes, which inherently limit the number of supported users due to orthogonal resource allocation. The progression of multiple access technologies in cellular networks has led to revolutionary changes in each generation, requiring substantial performance enhancements [4]–[6].With the advent of 5G in 2020, NOMA became the first non-orthogonal MA technology, designed to improve spectral efficiency, connectivity, and performance [7].

Traditional OMA schemes are now insufficient to address the increasing demand for high-speed, low-latency, and energy-efficient wireless communication networks, necessitating improvements in multiple access techniques. Additionally, the growing integration of IoT and mobile Internet applications further intensifies the need for an efficient multiple access strategy that supports large-scale connectivity [8]. In response, Non-Orthogonal Multiple Access (NOMA) has emerged as a key enabling technology for 5G and beyond wireless communication systems, addressing the growing demand for high spectral efficiency, low latency, and massive connectivity. In NOMA, multiple users are distinguished at the receiver based on differences in either their power levels or their unique spreading codes. The two primary categories of NOMA are Power-Domain NOMA (PD-NOMA), which relies on superposition coding (SC) at the transmitter and successive interference cancellation (SIC) at the receiver [9] - [11]. However, as the number of users increases, SIC becomes computationally complex, posing a scalability challenge. The Code-Domain NOMA (CD-NOMA) distinguishes users using unique spreading codes, similar to Direct Sequence-Code Division Multiple Access (DS-CDMA). Allows multiple users to share the same frequency, time, and code resource blocks through unique signature codes. A notable example of CD-NOMA is Interleave Division Multiple Access (IDMA), which has garnered attention as a promising 5G communication standard due to its ability to overcome multiple access interference (MAI) and inter-symbol interference (ISI) [12], [13].

IDMA is a special variant of CDMA that enhances system performance by employing chip-level interleaving rather than assigning a unique signature code to each user. The key advantage of IDMA is its ability to mitigate interference, thus improving system reliability [14]. Several companies have proposed different CD-NOMA schemes, which include Interleave Grid Multiple Access (IGMA) by Samsung, Repetition Division Multiple Access (RDMA) by MediaTek, and IDMA by Nokia. In IDMA, the interleaving mechanism rearranges input data sequences at the transmitter, breaking low-weight input sequences and increasing the code-free Hamming distance. This restructuring minimizes interference and improves error correction. At the receiver, a de-interleaver restores the original sequence, making the correlated noise appear statistically independent. This enhances the system’s ability to

correct transmission errors [15]–[17]. Despite its advantages, existing IDMA's suffer from two major limitations that affect their performance, namely, interleaver design, Choosing an optimal interleaver is crucial for minimizing interference and ensuring robust signal detection and Forward Error Correction (FEC) coding. Selecting an efficient FEC technique is essential to enhance system reliability and reduce error rates. This research aims to enhance the performance of IDMA by integrating Gold Sequence Interleavers in tandem with Low-Density Parity-Check (LDPC) coding to improve the reliability and efficiency in 5G wireless systems.

2. Literature Review

In recent decades, numerous researchers have focused on evaluating the performance of advanced multiple access and error correction techniques to enhance the efficiency of wireless communication systems. This section will explore the different methods and algorithms that have been adopted by previous researchers to enhance the efficiency and reliability of wireless communication systems.

In [18], a hybrid OFDM-IDMA system was investigated, incorporating polar coding as the forward error correction technique and a Gold code-based interleaver. The approach aimed to enhance bit error rate (BER) performance for a system with 10 users and normalized carrier frequency offsets (CFO) ranging from 0.1 to 0.5. Simulations were conducted in the presence of both Rayleigh fading and AWGN channels, utilizing 64-QAM modulation. A modified successive interference cancellation (SIC) algorithm was introduced for multi-user detection to mitigate multiple access interference. The results demonstrated that for a normalized CFO of 0.1 with 10 users at an SNR of 15 dB, the proposed system achieved a BER improvement to 1.021×10^{-4}. The research primarily focused on a fixed number of users (10) and specific normalized CFO values (0.1 to 0.5), limiting its generalizability to larger user loads and varying CFO conditions.

The research of [19] examined the performance of the Multiplicative Interleaving with Tree Algorithm (MITA) interleaver for grouped IDMA systems, specifically SCFDMA-IDMA and OFDM-IDMA, using QPSK modulation over a powerline channel. The primary objective was to evaluate the MITA algorithm in terms of complexity and throughput across multiple communication systems to determine its suitability for 5G technology. Higher throughput and lower complexity were achieved due to the structure of the MITA interleaver, which allocated more users per clock cycle compared to existing interleavers such as random, tree, and FLRITI. The analysis was conducted in a MATLAB environment, considering varying parameters such as data length and user count, with results plotted in terms of bit error rate (BER). Additionally, the effect of convolutional coding on grouped IDMA systems was examined, followed by a complexity comparison. The simulation results demonstrated that the MITA interleaver outperformed FLRITI in BER performance, particularly for a large number of users, with its efficiency improving as the user count increased. Furthermore, the complexity comparison indicated that MITA exhibited lower computational complexity than FLRITI. However, the evaluation is limited to QPSK modulation and powerline channels, leaving its effectiveness in higher-order modulations and diverse wireless environments unexplored.

The work of [20] proposed a bio-inspired approach to enhance the performance of an OFDM-IDMA system. To improve BER performance in a multiuser environment with CFOs, the SIC-MUD and SIC-MUD with SU-LA algorithms were introduced. The SIC-MUD technique mitigated the impact of multiple access interference (MAI), while the SU-LA algorithm optimized pilot positions to enhance channel estimation accuracy. The integration of these algorithms reduced estimation errors, achieving a mean squared error (MSE) of 0.0472. Simulations were conducted using CFO values of 0, 0.1, and 0.2, with 1, 4, and 8 users under a Rayleigh

channel and employing 16-QAM modulation. The results demonstrated that, compared to the SIC-MUD algorithm, the proposed approach improved BER by 41.17% and effectively tolerated a 0.1 CFO in the presence of 8 users. Additionally, the second-order regression model based on Response Surface Methodology (RSM) exhibited an R^2 value of 91.35%, accurately predicting the system's response. The improves BER performance in an OFDM-IDMA system, but it is limited to specific CFO values (0, 0.1, 0.2) and user counts (1, 4, 8), restricting its applicability to larger-scale networks.

[21] Examined the performance of interleave division multiple access (IDMA)-based random access with different interference canceller structures to support massive machine-type communications (mMTC) in the fifth-generation (5G) mobile communication system. To enable massive connectivity in the uplink, a grant-free and contention-based multiple access scheme was considered essential for reducing control signaling overhead and transmission latency. To mitigate packet loss caused by collisions and facilitate multi-packet reception, non-orthogonal multiple access (NOMA) with interference cancellation at the base station receiver was employed. IDMA was utilized, and various interference canceller structures, including the parallel interference canceller (PIC), successive interference canceller (SIC), and their hybrid, were compared in terms of error rate and decoding delay time. Through extensive computer simulations, the findings demonstrated that IDMA-based random access was a viable approach for supporting mMTC, and the PIC-SIC hybrid provided an effective balance between error rate and decoding delay time. However, the study is limited to specific interference canceller structures and does not explore the impact of varying traffic loads and real-world channel impairments on IDMA-based random access.

In [22], a hardware architecture was developed to decode (N, K) polar codes using a low-density parity-check (LDPC) code-like decoding approach. By applying suitable pruning techniques to the dense graph of the polar code, the decoder architecture was optimized with a reduced number of check nodes (CN) and variable nodes (VN). Pipelining was incorporated into the CN and VN architectures, effectively minimizing the critical path delay. Further reduction in latency was achieved through a fully parallelized, single-stage architecture, in contrast to the log N stages required in the conventional belief propagation (BP) decoder. The designed decoder, intended for short-to-intermediate code lengths, was implemented on a Virtex-7 field-programmable gate array (FPGA), achieving a throughput of 2.44 Gbps, which was four times higher than that of the fast-simplified successive cancellation decoder and 1.4 times higher than the combinational decoder. The proposed decoder for the (1024, 512) polar code demonstrated a negligible bit error rate (BER) of 10^{-4} at 2.7 Eb/No (dB) and converged more rapidly than the BP decoding scheme on a dense parity-check matrix. Additionally, the decoder was implemented on a Xilinx UltraScale FPGA and validated against the 5G New Radio physical downlink control channel specification. However, the performance in high-noise environments and scalability for longer polar codes was unaddressed.

The research of [23] presented a novel approach to enhance system performance in a multiple access channel (MAC) through power allocation and the design of low-density parity-check (LDPC) codes. Power profiles were determined using a data optimization method based on maximizing mutual information. The Gaussian approximation (GA) method was employed to approximate the probability density function (PDF) of messages, and message updating formulas were derived. Optimized power and degree profiles were obtained for a two-user scenario. At the receiver end, the detector and decoder exchanged extrinsic information iteratively. Three cases were compared under a spectral efficiency of 0.5. Simulation results demonstrated that a performance gain of 0.8 dB was achieved compared to optimizing only the LDPC code. The

study was limited to optimizing power allocation and LDPC code design for a two-user MAC scenario, but it does not explore scalability to more users or real-world channel impairments.

3. Methodology

This section discusses the steps and methods used in the performance evaluation of Interleaved Division Multiple Access (IDMA) incorporating Low-Density Parity-Check (LDPC) forward error correction codes for 5G wireless systems. The proposed system is designed to optimize error correction performance while maintaining efficiency in 5G systems.

3.1 Interleave Division Multiple Access Framework

In an Interleave Division Multiple Access (IDMA) system, each user is allocated a unique interleaver, which serves as the primary means of user separation in contrast to conventional multiple access techniques that rely on orthogonal spreading codes. The chip-level interleaving mechanism, analogous to Direct Sequence Code Division Multiple Access (DS-CDMA), ensures that the transmitted sequences from distinct users exhibit minimal cross-correlation, thereby mitigating multi-user interference (MUI) and enhancing system robustness against fading and interference. As depicted in Figure 1, the fundamental framework of an IDMA system consists of three principal components: a transmitter, a multiple-access channel, and a receiver.

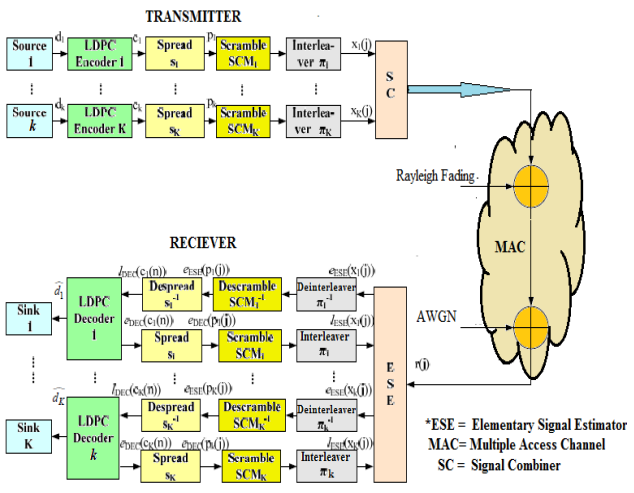

Figure 1. LPDC-IDMA Framework

3.1.1 Transmitter

The information data from user k is first encoded at the transmitter side by a forward error control (FEC) encoder, denoted as ENC. In this study, the FEC used is LDPC. The input data sequence is passed through the encoder at rate R, employing a low-rate code C. The data is processed in blocks of size N information bits for each user k is given as equation (1).

$$d_k = [d_1,\ d_2,\ d_3\ \ldots\ldots\ldots\ldots\ldots d_{k,}\ ] \qquad (1)$$

The data sequence encoded is represented in equation (2) as:

$$b_k = [b_k(0),\ \ldots\ldots\ldots\ldots\ldots b_{k,}\ (N_e - 1)]^T \qquad (2)$$

This research adopted the QPSK modulation for simplicity. The k^{th} bit data sequence $d_k(n)$, in the input data stream $d(n)$ from k^{th}-user is encoded by an LDPC encoder. This generates $c_k(n)$ for k = 1, 2,…,L, where L is the frame length. The k^{th} coded bit from user-k, $c_k(n)$ is spread by length-N spreading sequence $s(n)$ in the form $c_k(n) \rightarrow c_k(n)s(n)$. So, the chip sequence obtained after spreading as {ci(n) ∈{+1,−1},i = 1,2,…,i}, where I= N×L is the frame length. A chip-level interleave π(k) is then applied to produce the transmitted signals { xi(n) ,i = 1,2,…,i}. The coding rate is expressed in equation (3) as:

$$R_1 = \frac{N_i}{N_c} \qquad (3)$$

Where b_k denotes given bit, N_i is the number of input bits and N_c is the number of output bits. Each bit, b_k is again encoded using a low rate code such as a spread encoder with a rate given in equation (4) as:

$$R_2 = \frac{1}{S_{pk}} \qquad (4)$$

Where S_{pk} denotes the spreading factor. So, the overall code rate which produces a chip signal is given in equation (5) as:

$$R = \frac{R_1}{R_2} \qquad (5)$$

For the purpose of user separation, the output of the second encoder is fed right into the user unique interleaver $(\pi_1, \pi_2\ \ldots \pi_k)$, this generates:

$xk(j)$ for j = 1,2……..j. Where; j denotes the user frame length. The interleaver is used to permute the input data and then rearrange it using gold sequence pattern in [24]. It discriminates among different IDMA users, resulting in the $xk(j)$ sequence usually called "chips". The resulting signal is then routed across the various access channels.

3.1.2 Channel

After transmission, the sequence x_k propagates through the communication channel, where it experiences path loss, as well as both long-term and short-term fading. In this study, we assume the channel follows a Rayleigh fading model. In addition to these fading effects, the signal is also impacted by interference from other users (multiuser interference) and additive white Gaussian noise (AWGN), contributing to multiple access interference (MAI) and noise at the receiver. The transmitted signal $x_k(j)$ is then affected by the corresponding channel coefficient $h_k(j)$ which represents the channel's effect on the signal. This results in the received sequence being expressed as $x_k(j)$. $h_k(j)$. $h_k(j)$ Denotes the channel coefficient, which accounts for the combined effects of both fading channel effects along with the power control of user-k [24]. For analytical tractability, the channel coefficient h_k is assumed to be real-valued; however, the results can be readily extended to complex-valued channels. The transmitted sequence x_k propagates through a flat fading channel, where the received signal is given by $x_k(j)$. $h_k(j)$. This signal is subject to multiple impairments, including inter-user interference from other simultaneously active users and additive white Gaussian noise (AWGN). Consequently, the received signal at the receiver can be expressed in equation (6) as:

$$s(j) = \sum_{k=1}^{k} x_k(j) \,.\, h_k(j) \tag{6}$$

By assuming $\boldsymbol{\delta}_A\,(j)$ as samples of a zero-mean AWGN the signal suffers just before the receiver which has variance as in equation (7) as follows [25]:

$$\sigma^2 = \frac{N_o}{2} \tag{7}$$

AWGN has probability density function shown in equation (8)

$$p(x) = \frac{1}{\sqrt{2\pi\sigma^2}} e^{\frac{-(x-\mu)^2}{2\sigma^2}} \tag{8}$$

In a Rayleigh fading channel model, the transmitted radio signal undergoes scattering due to multiple surrounding objects, causing multipath propagation between the transmitter and receiver. This model is particularly applicable in scenarios where there is no dominant line-of-sight (LoS) component between the communicating terminals. The signal amplitude variations over the channel are assumed to follow a Rayleigh distribution, which characterizes the statistical behavior of the received signal in a rich-scattering environment. Mathematically, Rayleigh fading is modeled as the envelope of a signal comprising two independent and identically distributed (i.i.d.) Gaussian random variables representing the in-phase and quadrature components. The resultant signal magnitude follows a Rayleigh distribution, making this model suitable for environments where the received signal consists purely of scattered and reflected multipath components without a direct LoS component [26][27].

Now considering a circularly symmetric complex Gaussian random in equation (9):

$$Z = X + jY \tag{9}$$

Where X and Y denote the real and imaginary components respectively Gaussian random variables having the same distribution and zero mean. The circularly symmetric complex random variable Z is presented in equation 10.

$$E(Z) = E\left|e^{j\theta}\, Z\right| = e^{j\theta}\, E|Z| \tag{10}$$

The variance of a Gaussian random variable with a circularly symmetric complex (SSC) specifies its statistics which is denoted by equation 11.

$$\sigma^2 = E|Z^2| \tag{11}$$

The random variable Z is the signal amplitude. So, the Rayleigh fading distribution with magnitude

mode |Z|, with probability density function (PDF) is denoted by equation 12.

$$P_{ray}(Z) = \frac{Z}{\sigma^2} e^{\frac{-z^2}{2\sigma^2}} \quad Z \geq 0 \tag{12}$$

Here σ^2 is the variance of the in-phase and quadrature components. All signals have almost the same attenuation but arrive at the receiver with various phases. This model, known as the Rayleigh fading channel model, is suitable for situations involving a high number of reflectors [27]. The received signal is presented in equation (13) as:

$$S(j) = \sum_{k=1}^{k} x_k(j) h_k(j) + \boldsymbol{\delta}_A(j) \tag{13}$$

3.1.3 Receiver

The received signal is processed by a multi-user detection (MUD) receiver, which consists of an elementary signal estimator (ESE) and a bank of *K*single-user decoders (DECs), each based on a posteriori probability (APP) decoding for individual users employing Gold codes. The APP decoder is responsible for recovering messages that were encoded using the Gold sequence encoder. The ESE algorithm is implemented through a set of functional blocks that constitute the ESE subsystem. It primarily mitigates multiple access interference (MAI) by employing a chip-by-chip detection strategy. Multiple access and coding constraints are iteratively addressed within the ESE and DECs, ensuring an efficient decoding process. The extrinsic information exchange between the $ESE[eESE(x_k(j))]$ *and* $DECs[eDEC(x_k(j))]$ forms the basis of an iterative detection framework, where the ESE performs chip-by-chip detection to refine signal estimates. The ESE output $[eESE(x_k(j))]$ is initially passed through the de-interleaver corresponding to the k-th mobile user. The de-interleaver reorders the received elements to restore the original sequence, following the Gold code sequence permutation. This operation ensures the correct reconstruction of the transmitted data sequence. Finally, the receiver's de-spreader performs the inverse operation of the transmitter's spreading process, effectively recovering the original transmitted signal before further processing. After the de-interleaving process, the extrinsic data from the ESE serves as a priori information for the k-th decoder (DEC) corresponding to user k. The output of the k-th DEC, after undergoing interleaving, provides updated extrinsic data $[eESE(x_k(j))]$ for the subsequent iteration. This process is repeated multiple times until a final hard decision (d_k) is made on the information bits (d_k) [28].

The chip-by-chip detection technique is summarized below from equation (14) – (12) [29] [30]:

Initialization

$$e_{DEC}(x_k(j)) = 0 \qquad \forall k, j \tag{14}$$

Iterative process

$$\mu_k = \tanh\frac{e_{DEC}(x_k(j))}{2} \qquad \forall k, j \tag{15}$$

$$var_k(j) = 1 - (\mu_k(j))^2 \qquad \forall k, j \tag{16}$$

$$E\{r(j)\} = \sum_{k=1}^{K} h_k \mu_k(j) \qquad \forall j \tag{17}$$

$$Var\{r(j)\} = \sigma_n^2 + \sum_{K=1}^{K} (h_k)^2 Var_k(j) \qquad \forall j \tag{18}$$

$$E\{\varepsilon_k(j)\} = E\{r(j)\} - h_k \mu_k(j) \qquad \forall k, j \tag{19}$$

$$Var\{\varepsilon_k(j) = Var\{r(j)\} - (h_k)^2 Var_k(j) \qquad \forall k, j \tag{20}$$

$$\tilde{\imath}_{\text{ESE}} x_k(j) = Log\left(\frac{P_r(x_k(j) = +1}{P_r(x_k(j) = -1}\right) \qquad \forall k, j \tag{21}$$

$$e_{ESE}(x_k(j)) = 2_{hk} \text{X} \frac{r(j) - E(\varepsilon_k(j))}{Var(\varepsilon_k(j)} \qquad \forall k, j \tag{22}$$

The probability that $x_k(j)t$akes the value +1 is represented as $P(x(j) = +1)$ while $P(x(j) = -1)$ denotes the probability of $x_k(j)$ assuming the value of -1. The ESE (Extrinsic Soft-Estimate) receiver consists of a bank of outputs, denoted as $e_{ESE}(x_k(j))$ is illustrated in figure 1. The ESE receiver processes two primary inputs: j which represents the received signal, and a set of feedback inputs, $\tilde{\imath}(x_k(j))$ which contain the log-likelihood ratios (LLRs) of$x_k(j)$. Equation (19) assumes a Gaussian distribution for these values, characterized by a specific mean and variance [31]. The outputs from the ESE undergo a de-interleaving process to obtain $\tilde{\imath}(x_k(j))$, which are then forwarded to the corresponding decoders. Each decoder produces two types of outputs: hard and soft decision outputs (HSO and SDO). These outputs help refine the LLR values of $x(j)$

through a feedback mechanism. The FB process includes a re-interleaving step, where $\tilde{\imath}(x_k(j))$ is used to generate updated intrinsic information about$x_k(j)$. which is then fed back into the ESE. This iterative procedure continues until the system reaches the desired bit error rate (BER). The complete receiver process is visually represented in the flowchart of Figure 2.

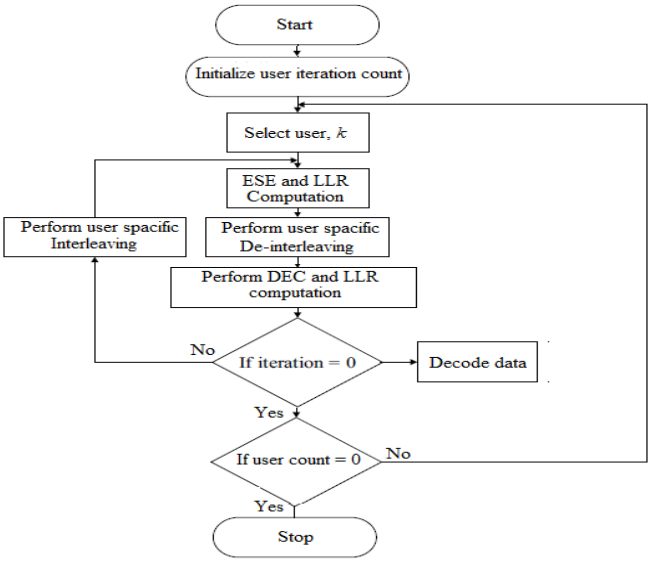

Figure 2. The IDMA Iterative Decoding

Ultimately, after the last operation, the necessary data information to decode $e_{ESE}(x_k(j))$ is obtained, the decoder then computes the extrinsic log-likelihood ratios (LLR). Once $e_{DEC}(x_k(j))$ decoding is completed, the calculations of equation (15) in equation (20) are repeated.

3.2 Additive White Gaussian Noise Mathematical Model

The Additive White Gaussian Noise (AWGN) model represents a fundamental noise process in wireless communication systems and is crucial for evaluating the performance of various multiple-access techniques, including Interleaved Division Multiple Access (IDMA) in wireless networks. The AWGN channel introduces noise with a Gaussian amplitude distribution and a flat spectral density across all frequencies, making it a suitable approximation for thermal noise in communication systems. The AWGN model assumes that the received signal, which is the sum of the transmitted signal and a noise component, is given by equation (23) [32].

$$y(t) = x(t) + n(t) \tag{23}$$

The probability density function (PDF) of the noise sample n follows a Gaussian distribution given by equation (24).

$$p(n) = \frac{1}{\sqrt{2\pi\sigma^2}} e^{\frac{-n^2}{2\sigma^2}} \tag{24}$$

Where $\sigma^2 = \frac{N_o}{2}$

The power spectral density (PSD) of AWGN is constant and given by equation (25).

$$S_n(f) = N_o \tag{25}$$

In communication systems, the Signal-to-Noise Ratio (SNR) is an important metric used to quantify the level of signal power relative to the noise power. It is presented in equation (26) as [33]:

$$SNR = \frac{P_s}{P_n} = \frac{E_b}{N_o} \tag{26}$$

Where P_s denotes signal power, P_n is noise power, E_b is energy per bit and N_o is noise power spectral density.

The bit error rate (BER) of AWGN is presented in equation (27).

$$BER = Q\left(\sqrt{\frac{2E_b}{N_o}}\right) \tag{27}$$

Where Q denotes Q-function, representing the tail probability of the Gaussian distribution, and E_b/N_o is the energy-per-bit-to-noise-power spectral density ratio.

3.3 Rayleigh Mathematical Model

The Rayleigh fading model is commonly used in wireless communications to characterize the rapid amplitude fluctuations of signals caused by multipath propagation. This model is particularly applicable in environments where there are no line-of-sight (LOS) conditions, such as urban areas with many obstacles. In a Rayleigh fading channel, the envelope of the received signal

follows a Rayleigh distribution, given by equation (28) [34].

$$r\ (t) = s(t).h(t) + n(t) \quad (28)$$

Where $s(t)$ denotes the transmitted signal, $h(t)$ is multipath fading coefficient and $n(t)$ is Additive white Gaussian noise. The multipath fading coefficient $h(t)$ is expressed by equation (29) as:

$$h(t) = \sqrt{X(t)^2 + Y(t)^2} \quad (29)$$

Where $X(t)$ and $Y(t)$ are independent Gaussian random variables with zero mean and equal variance σ^2. In the probability density function (PDF), the amplitude of the Rayleigh fading signal $r(t)$ follows the Rayleigh distribution, and is given by equation (30) as:

$$p(r) = \frac{r}{\sigma^2} e^{\frac{-r^2}{2\sigma^2}}, \quad r \geq 0 \quad (30)$$

Where σ^2 is the variance of the underlying Gaussian random variable. The cumulative density function (CDF) is expressed in equation [31] as:

$$p(R \leq r) = 1 - e^{\frac{-r^2}{2\sigma^2}}, \quad r \geq 0 \quad (31)$$

The average power of the received signal in a Rayleigh fading environment is expressed in equation (32) as:

$$\mathrm{E}[|r|^2 = 2\sigma^2 \quad (32)$$

In Rayleigh fading environments, the SNR is affected by the fading. The SNR at the receiver is expressed in equation (33) as:

$$SNR = \frac{P_S}{P_n}.|h|^2 \quad (33)$$

Where P_s denotes signal power, P_n is noise power and $|h|^2$ follows an exponential distribution with mean.

For different modulation schemes, the Bit Error Rate (BER) can be analyzed under Rayleigh fading conditions. This research adopted the QPSK modulation in a Rayleigh fading channel, the average BER is expressed in equation (34) as:

$$BER = \frac{1}{2}.e^{\frac{-E_b}{N_o}} \text{ (For Large SNR)} \quad (34)$$

Where E_b is energy per bit and N_o is noise power spectral density.

3.4 Simulation Setup

In this research, the parameters in the Table 1, were carefully selected to evaluate the performance of Interleaved Division Multiple Access (IDMA) with Low-Density Parity-Check (LDPC) codes in a 5G wireless system. A user count of 40 demonstrates IDMA's capability to handle multiple users efficiently. The carrier frequency of 2 GHz, typical for 5G, offers a realistic propagation environment. Quadrature Phase Shift Keying (QPSK) modulation balances spectral efficiency and robustness. The inclusion of both AWGN and Rayleigh channels allows assessment under noise and multipath fading conditions, respectively, while ideal channel estimation isolates the coding gain of LDPC. Gold codes for interleaving ensure effective user separation, crucial for IDMA. An information block length of 1024 bits and a code rate of 0.5 are chosen to optimize error correction performance without excessive redundancy. A spreading sequence adopted for the encoded information bits was [+1, -1, +1, -1, -1]; furthermore, a spreading factor of 16 enhances multiple access capability, while a data length of 1024 bits and a block length of 2000 bits simulate typical 5G packet sizes. The 15 decoding iterations ensure sufficient LDPC convergence, and comparison with random, convolutional, and tree interleavers, as well as turbo codes, provides insights into IDMA's efficiency relative to other schemes. Lastly, a user data rate of 1/16 bits per symbol reflects the high-density user scenarios expected in 5G networks, emphasizing the importance of robust FEC in maintaining data integrity.

Table 1. Parameters Used for the System Simulation.

Parameter	Value
Number of users	40
Carrier frequency	2 GHz
Modulation type	QPSK
Channel	AWGN, Rayleigh

Channel estimation	Ideal
FEC type	LDPC
Interleaver code sequence	Gold codes
Information block length	K=1024
Code rate	R_c= 0.5
Spreading factor	S = 16
Data length	M =1024
Number of iterations	15
Block length	N = 2000
Comparison interleavers	Random, Convolutional and Tree
Other comparison FEC	Turbo code
User data rate	R = 1/16 Bits per symbol

In this research, figure 3 depicts the simulation model for the Gold interleaver with AWGN. The components include a Gold Sequence Generator for user separation, an LDPC Encoder/Decoder for error correction, and a General Block Interleaver for mitigating burst errors. The channel model includes AWGN (Additive White Gaussian Noise) to simulate real-world transmission conditions, while Error Rate Calculation modules analyze Packet Error Rate (PER) and LDPC Bit Error Rate. Additionally, the SNR and RX Constellation blocks assess signal quality and system performance under various noise conditions.

Furthermore, figure 4. Shows the simulation model of the Gold interleaver with REYLEIGH. The key components include a Gold Sequence Generator for user separation, an LDPC Encoder/Decoder for enhanced error correction, and a General Block Interleaver to mitigate burst errors. The system incorporates a Rayleigh SISO (Single Input Single Output) Fading Channel, modeling the multipath fading effects encountered in real-world wireless environments. Error Rate Calculation modules analyze Packet Error Rate (PER) and LDPC Bit Error Rate, while SNR and RX Constellation assess system performance and signal quality. This setup helps evaluate IDMA's robustness in handling fading channels, improving reliability, and optimizing transmission efficiency in 5G networks.

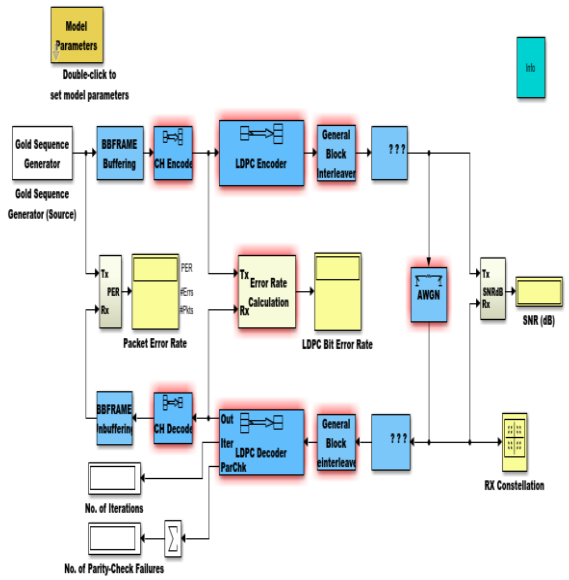

Figure 3. Gold interleaver with AWGN

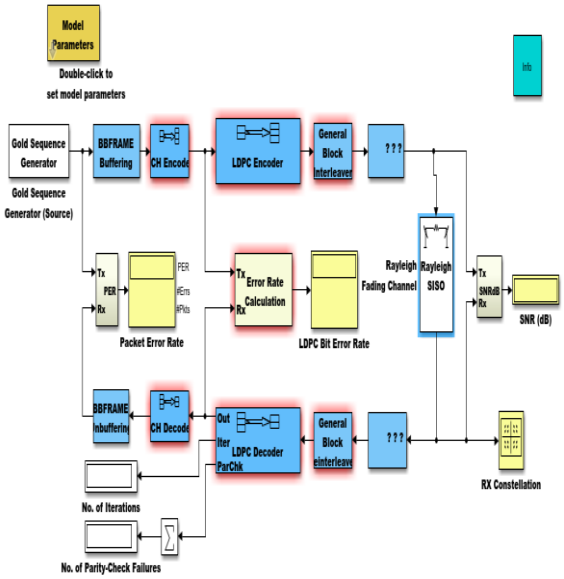

Figure 4. Gold interleaver with REYLEIGH

3.5 Performance Metrics

The Bit Error Rate (BER) and Signal-to-Noise Ratio (SNR) are critical performance metrics adopted in this research to evaluate Interleaved Division Multiple Access (IDMA) with Low-Density Parity-Check (LDPC) Forward Error Correction (FEC) in 5G wireless systems. BER,

defined as the ratio of erroneous bits to the total transmitted bits, provides a direct measure of system reliability and the effectiveness of LDPC decoding in mitigating channel impairments, particularly in multipath fading and interference-prone environments. SNR, expressed in decibels (dB), represents the ratio of signal power to noise power and serves as a key indicator of link quality, decoding efficiency, and overall system robustness. These two metrics are chosen because IDMA relies on iterative multi-user detection (MUD) and LDPC decoding, where system performance is heavily influenced by noise, interference, and error correction capability. BER versus SNR curves provide insights into how well the system can tolerate interference and recover from errors across AWGN and Rayleigh fading channels, essential for evaluating error correction efficiency, spectral efficiency, and system capacity in high-density 5G user scenarios. Mathematically, the BER and SNR are expressed in equations (35) and (36), respectively.

$$BER = \frac{Number\ of\ Error\ Code\ in\ Transmission}{Total\ Number\ of\ Code} \text{ x } 100\% \quad (35)$$

$$SNR = 10Log_{10}\frac{Signal\ Power}{Noise\ Power}\ (dB) \quad (36)$$

4 Result

This section presents the performance evaluation of the developed LDPC-IDMA scheme, where all simulations were executed in MATLAB R2022a using a QPSK modulation scheme and system parameters detailed in Section 3.4. The analysis focused on key performance metrics such as Bit Error Rate (BER) and Signal-to-Noise Ratio (SNR) to rigorously assess the system's robustness and error-correcting capabilities under varying noise conditions. The LDPC-IDMA framework, which integrates low-density parity-check codes with interleaved division multiple access for enhanced wireless systems, was benchmarked against a turbo-coded system operating over the same channel.

4.1 Simulation Result of the LDPC-IDMA for 5G-NOMA System

Starting with the MATLAB-generated constellation diagram for quaternary phase-shift keying (QPSK), where the horizontal axis represented the in-phase component and the vertical axis the quadrature amplitude, the diagram's points clearly indicated the modulation order. The equalized QPSK signal constellation, which mapped each pair of input bits (or integers) to its corresponding constellation symbol according to a predefined ordering, was visually confirmed, thereby validating the mapping block's functionality. A discrete-time signal trajectory scatter plot of the modulated signal further illustrated the QPSK system's modulation characteristics, including signal pulse behavior and any inherent distortions, which were critical for verifying the designed model's performance. Additionally, Figure 5 presents the Rayleigh fading channel output excluding the phase component of the equalized QPSK discrete-time signal trajectory, offering insight into the channel-induced distortions affecting the constellation and highlighting the system's robustness under realistic fading conditions.

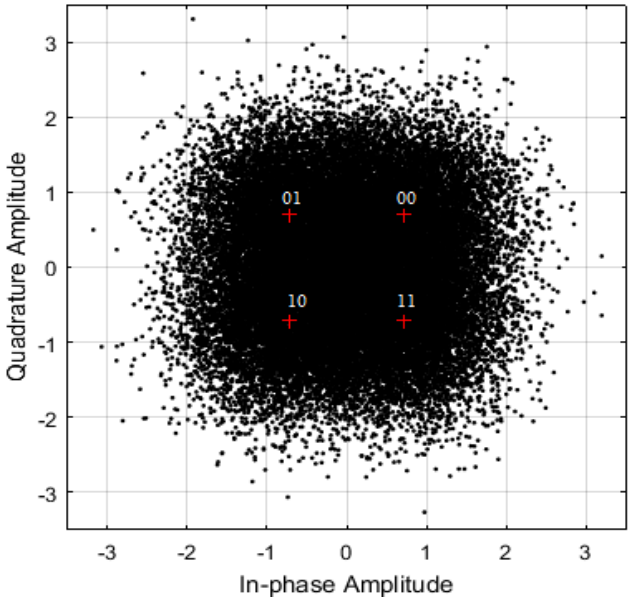

Figure 5. Constellation Diagram for QPSK

To achieve improved SNR and BER performance, it was imperative that the estimated spread spectrum value closely matched the actual value. The relationship between BER and SNR was computed by comparing the total number of bits received at the receiver against the number of erroneous bits introduced by channel impairments, such as multipath fading and phase noise. This necessitated an optimal receive sequence to mitigate the imperfections present in both the transmitter and receiver oscillators. Additionally,

the introduction of Additive White Gaussian Noise (AWGN) to the Rayleigh fading channel output further degraded the signal, resulting in a noisy, faded QPSK constellation, as depicted in figure 6.

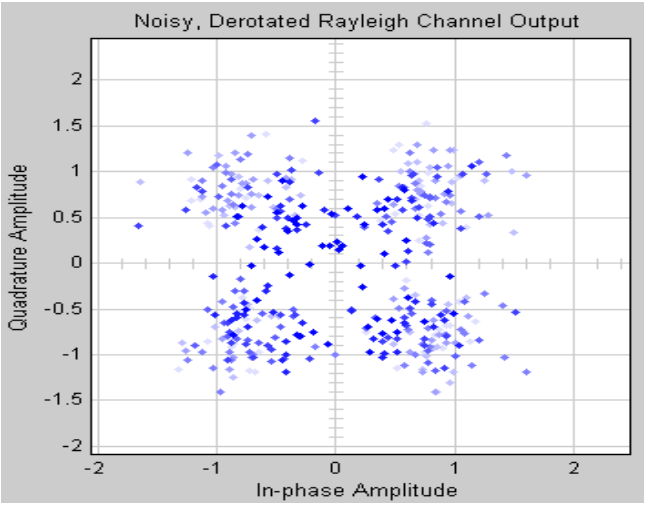

Figure 6. The Noisy Faded QPSK Received Spread Spectrum Signal

Figure 7 displays the power of the faded signal versus the number of samples for the signal that encounters Rayleigh fading impairment in the channel.

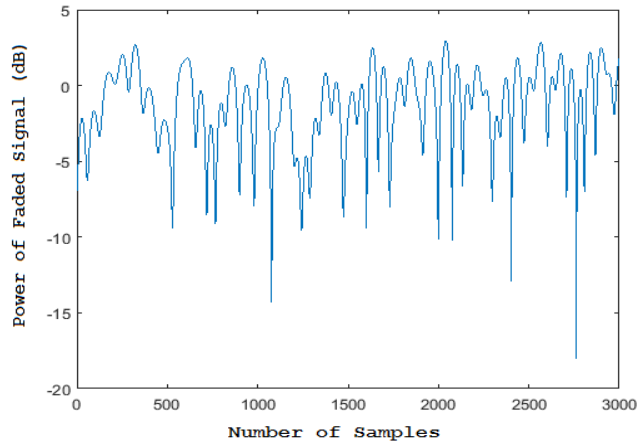

Figure 7. Faded Signal Power versus Number of Samples for the Rayleigh Fading Channel.

4.2 Simulation of BER Performance against SNR Effects

Considering an identical Bit Error Rate (BER) performance requirement for all users and the utilization of the same Low-Density Parity-Check (LDPC) forward error correction (FEC) code, the study evaluated the performance of Interleave-Division Multiple Access (IDMA) and Code-Division Multiple Access (CDMA) under identical conditions. The simulation incorporated a system with 40 active mobile users subjected to a Rayleigh fading channel combined with additive white Gaussian noise (AWGN), where the energy per bit to noise power spectral density ratio E_b/N_o varied dynamically. The IDMA scheme, which leveraged iterative multi-user detection and LDPC decoding, demonstrated superior BER performance compared to CDMA, which employed stringent power control and advanced interference cancellation. The results, detailed in Table 2, confirmed that IDMA with LDPC effectively mitigated multi-user interference (MUI) and improved decoding efficiency, outperforming CDMA under the given conditions.

Table 2. Result of BER against Eb/No for 10 Users for Both IDMA and CDMA

S/N	E_b/N_o(dB)	BER (dB)	
		CDMA	IDMA
1	1.0000	0.0408231	0.0307120
2	2.0000	0.0394211	0.0254019
3	3.0000	0.0326009	0.0226011
4	4.0000	0.0300100	0.0173110
5	5.0000	0.0277009	0.0142019
6	6.0000	0.0188010	0.0088041
7	7.0000	0.0121100	0.0051017
8	8.0000	0.0080100	0.0018012
9	9.0000	0.0026101	0.0004015

From Figure 8, it is evident that the Bit Error Rate (BER) performance of the proposed 5G Gold code-based interleaver Low-Density Parity-Check (LDPC)-assisted Interleave-Division Multiple Access (IDMA) system significantly outperforms that of Code-Division Multiple Access (CDMA) in a Rayleigh fading channel with additive white Gaussian noise (AWGN). The enhanced BER efficiency of LDPC-IDMA is attributed to its iterative multi-user detection and interference suppression capabilities, which are further optimized by the structured interleaving properties of the 5G Gold code. Furthermore, as shown in Table 2, the deviation in BER performance between CDMA and IDMA at an energy per bit to noise power spectral density ratio (Eb/No) of 9 dB is:

$$Deviation = |0.002601 - 0.0004015| = 0.0021995dB$$

$$\%\ Improvement = \frac{0.0004015}{0.00219945} \text{x} \frac{100}{1} = 18.25\%$$

With an SNR improvement of about 0.0021995dB obtained for the case of IDMA and a better BER value, signifying that lower values of BER are obtained by the NOMA over the OMA scheme.

An SNR improvement of approximately 0.0021995dB was achieved with IDMA, resulting in better BER values. This demonstrates that the Non-Orthogonal Multiple Access (NOMA) scheme, leveraging the advantages of multi-user detection yields, lower BER compared to the Orthogonal Multiple Access (OMA) scheme. The improved performance of NOMA is attributed to its ability to efficiently manage interference while maintaining user fairness, even at lower SNR levels.

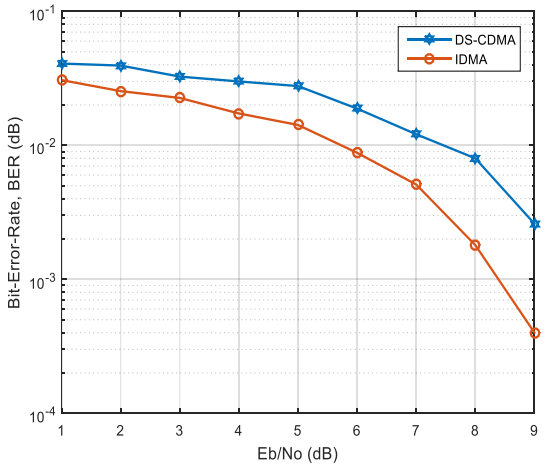

Figure 8. BER Performance Comparison of IDMA with CDMA

The IDMA system was simulated using Low-Density Parity-Check (LDPC) codes to demonstrate the enhanced error-correcting capabilities of LDPC FEC in reducing Bit Error Rate (BER) when subjected to both Additive White Gaussian Noise (AWGN) and Rayleigh fading channels. Table 3 presents the simulation results for BER performance under these channel conditions, comparing LDPC with Turbo coding at the same Eb/No value for 40 active mobile users. The results highlight the superior error correction efficiency of LDPC, particularly in handling channel impairments such as fading and noise. Furthermore, Figure 9 illustrates the comparative BER performance of the proposed LDPC-based FEC and Turbo code-based FEC, emphasizing the improved robustness of LDPC in maintaining lower BER under the same system conditions.

Table 3. IDMA BER Results for Rayleigh Fading Channel and AWGN for LDPC Compared with Turbo Coding for Same Value ofEb/No for 10 Users.

S/N	E_b/N_o (dB)	BER (dB) *RAYLEIGH FADING CHANNEL* LDPC TURBO	BER (dB) *AWGN* LDPC TURBO
0	0.0000	0.15991101 0.16001201	0.15771006 0.15800113
1	1.0000	0.01910042 0.01990006	0.00900151 0.01000064
2	2.0000	0.00300074 0.00400110	0.00080010 0.00101033
3	3.0000	0.00100063 0.00160046	0.00013085 0.00030171
4	4.0000	0.00031009 0.00061001	0.00003903 0.00009006
5	5.0000	0.00013083 0.00021034	0.00001139 0.00003204
6	6.0000	0.00010005 0.00017004	0.00000308 0.00000951
7	7.0000	0.00008001 0.00012023	0.00000119 0.00000402
8	8.0000	0.00006010 0.00010005	0.00000048 0.00000101
9	9.0000	0.00006001 0.00008003	0.00000009 0.00000030
10	10.000	0.00004082 0.00007011	0.000000088 0.00000020

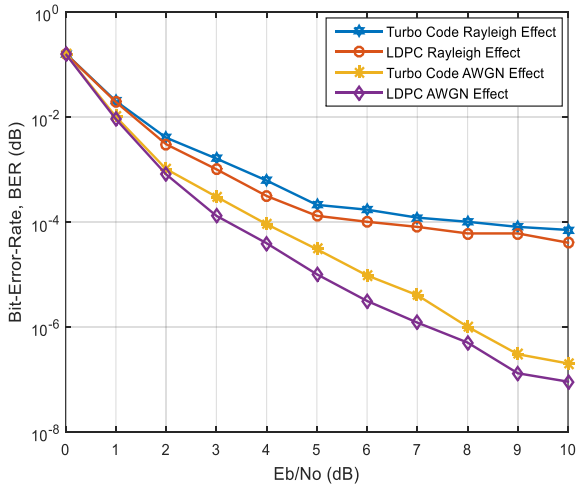

Figure 9. BER versus SNR Performance Comparison between the developed Gold Code IDMA LDPC based and Turbo code based FECs for 10 users over AWGN and Rayleigh Channels.

From Table 3 and Figure 9, the deviation between the turbo and LDPC for both Rayleigh fading and AWGN is computed:

Rayleigh fading:

For 9dB of Eb/No the BER deviation is:

$Deviation =$ | 0.00008003 - 0.00006001| = 0.00002002dB

AWGN:

For the same 9dB of Eb/No the BER deviation is:

$Deviation =$ | 0.00000030 - 0.00000009| = 0.00000021dB

An SNR improvement of approximately 0.00002002dB and 0.00000021dB was observed for the LDPC-coded system compared to the Turbo-coded system under both Rayleigh fading and AWGN conditions. This signifies that the LDPC code outperforms Turbo coding in terms of achieving lower BER values, particularly in challenging channel environments. The enhanced performance of LDPC can be attributed to its superior error-correcting capabilities, which effectively mitigate the effects of noise and fading through iterative decoding and sparse parity-check matrices. These results demonstrate that LDPC provides better error resilience, especially in scenarios involving high multi-user interference and complex fading channels.

The simulation result of the BER and SNR performance for the proposed gold sequence-based LDPC-IDMA system with different interleaver schemes, the random, convolutional, and tree interleavers, is presented in Table 4 and Figure 10, respectively.

Table 4. Result of BER against SNR for Different Interleavers

S/N	Eb/No(dB)	BER (dB)			
		GOLD	CONV	RANDOM	TREE
1	00.00	0.020054157	0.024437500	0.039541667	0.050150000
2	02.00	0.018900157	0.021595833	0.038566667	0.049508330
3	04.00	0.012595833	0.017313500	0.037360000	0.049354167
4	06.00	0.0102	0.0138	0.0367	0.0500
		79167	68333	58667	33333
5	08.00	0.009054167	0.010845833	0.035395833	0.050037500
6	10.00	0.005605833	0.007716661	0.035064167	0.050316667
7	12.00	0.004191667	0.005783333	0.034304167	0.049787500
8	14.00	0.002529167	0.003637500	0.033500000	0.049662500
9	16.00	0.001312500	0.001950000	0.033183333	0.049629167
10	18.00	0.001083333	0.001458333	0.032775001	0.059570833
11	20.00	0.000633333	0.000879167	0.032741667	0.050145833

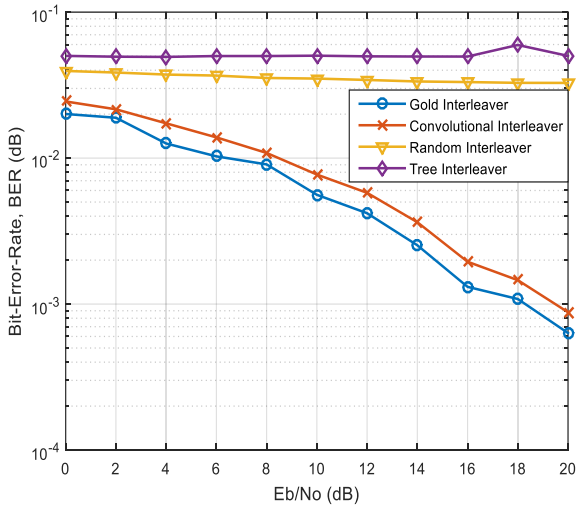

Figure 10. The BER Performance for Different Interleavers

The comparison of the gold sequence with convolution interleaver:

At 9dB of Eb/No the BER deviation is:

$Deviation =$ | 0.001950000 - 0.001312500| = 0.0006375dB

The comparison of the gold sequence with random interleaver:

At 9dB of Eb/No the BER deviation is:

$Deviation =$ | 0.033183333 - 0.001312500| = 0.031870833dB

The comparison of the gold sequence with tree interleaver:

At 9dB of Eb/No the BER deviation is

$Deviation =$ | 0.049629167- 0.001312500| = 0.048316667dB

From the comparison at 9dB Eb/No, the Gold sequence interleaver yields lower value of BER.

4.3 Discussion of Result

From Table 2 and Figure 8, it is evident that the Bit Error Rate (BER) for the same Energy per Bit to Noise Power Spectral Density Ratio (Eb/No) is significantly higher in Code-Division Multiple Access (CDMA) systems compared to the lower BER values recorded for the Interleave-Division Multiple Access (IDMA) system. Notably, the IDMA system demonstrated a Signal-to-Noise Ratio (SNR) improvement of approximately 0.0021995 dB, highlighting its superior BER performance over the Non-Orthogonal Multiple Access (NOMA) scheme in comparison to the conventional Orthogonal Multiple Access (OMA) scheme. Furthermore, Figure 9 presents a comparative BER analysis of the proposed Low-Density Parity-Check (LDPC) code-based Forward Error Correction (FEC) and the Turbo code-based FEC within the IDMA framework, employing a Gold Code interleaver. The evaluation was conducted with a fixed number of 40 users under both Additive White Gaussian Noise (AWGN) and Rayleigh fading channel conditions. The results clearly indicate that the LDPC-based FEC outperforms the Turbo-coded FEC, as evidenced by its consistently lower BER values. Specifically, an SNR improvement of approximately 0.00002002 dB and 0.00000021 dB was observed in the LDPC-coded system over the Turbo-coded system under Rayleigh fading and AWGN conditions, respectively. This confirms the superior error-correcting capability of LDPC codes in mitigating the effects of channel impairments compared to Turbo codes.

5. Conclusion

The performance of a 5G-NR IDMA system employing an LDPC coding scheme as its primary forward error correction (FEC) technique and a Gold code sequence interleaver was analyzed in this study. The evaluation of IDMA was necessitated to develop a system that met the fundamental requirements of 5G wireless communication. Previous research predominantly utilized Turbo coding as the FEC technique, while interleaving schemes such as random, convolutional, tree, and inverted tree interleavers were commonly employed. In this study, the Gold sequence interleaver was integrated with LDPC coding, and its performance was assessed in terms of bit error rate (BER) under various conditions. The BER versus Eb/No (energy-per-bit-to-noise-power spectral density ratio) analysis demonstrated that the CDMA exhibited a BER of 0.0026101, whereas the IDMA system achieved a BER of 0.0004015, representing an 18.25% improvement in error performance. Furthermore, the LDPC-IDMA system was evaluated under different link-level conditions, including Rayleigh fading and additive white Gaussian noise (AWGN) channels, with varying FEC schemes and interleaving techniques. The results indicated that the proposed Gold sequence interleaver, when integrated with LDPC, outperformed conventional interleaver designs—namely, random, convolutional, and tree interleavers—by achieving the lowest BER of 0.001312500 at 9dB.These findings demonstrated that the developed Gold sequence-based LDPC-IDMA system achieved near-optimal performance while maintaining a feasible level of system complexity for real-world implementation. Future research should explore alternative modulation schemes such as Gaussian minimum shift keying (GMSK) or quadrature amplitude modulation (QAM) to further enhance system performance. Additionally, advanced polar codes should be investigated as a potential primary FEC technique to operate in conjunction with the proposed Gold code sequence interleaver.

Reference

1. A. Solyman, and Yahya, Khalid. Evolution of wireless communication networks: from 1G to 6G and future perspective. International Journal of Electrical and Computer Engineering (IJECE). 2022, 12. 3943. 10.11591/ijece.v12i4.pp3943-3950.
2. M. Asghar, S. Memon, and J. Hämäläinen. Evolution of Wireless Communication to

6G: Potential Applications and Research Directions. Sustainability. 2022. 14. 6356. 10.3390/su14106356.

3. B. Panda, D. Senanayake, S. Gunathilake, and P. Singh. A Survey of Non-orthogonal Multiple Access for Internet of Things and Future Wireless Networks. Springer Nature. 2023, Pp. 199-210. https://doi.org/10.1007/978-3-031-47942-7_18.
4. S. A., Shuaibu, S. N., John, J. S., Mommoh, E., Noma-Osaghe, A. A., Ahmad, and H.I., Bulama. Development of an Adaptive Pathloss Prediction Model Using NeuroFuzzy Systems for Wireless Optimization in Urban Areas. International Research Journal of Engineering and Technology (IRJET). 2024, 11(12), 424 – 429. https://www.irjet.net/archives/V11/i12/IRJET-V11I1261.pdf.
5. A.R. Mishra. Fundamentals of Network Planning and Optimization 2G/3G/4G: Evolution to 5G, 2nd edn. Wiley, New York, 2018. ISBN: 9781119331711.
6. Solyman and K. Yahya. "Evolution of Wireless Communication Networks: From 1G to 6G and Future Perspective." International Journal of Electrical and Computer Engineering (IJECE), 2022, vol. 12, pp. 3943–3950. https://doi.org/10.11591/ijece.v12i4.pp3943-3950.
7. M.Z. Asghar, S.A. Memon, and J. Hämäläinen. "Evolution of Wireless Communication to 6G: Potential Applications and Research Directions." MDPI Journal of Sustainability, 2022, vol. 14, no. 6356. https://doi.org/10.3390/su14106356.
8. C. Teodorescu, A. Durnoi, and V. Vargas. "The Rise of the Mobile Internet: Tracing the Evolution of Portable Devices." Proceedings of the International Conference on Business Excellence, 2023, vol. 17, pp. 1645–1654. https://doi.org/10.2478/picbe-2023-0147.
9. Jehan, Ayesha & Zeeshan, Muhammad. (2022). Comparative Performance Analysis of Code-Domain NOMA and Power-Domain NOMA. Proceedings of the 2022 16th International Conference on Ubiquitous Information Management and Communication, IMCOM 2022, Pp 1-6. 10.1109/IMCOM53663.2022.9721725.
10. Mobasshir Mahbub, Raed M. Shubair, Contemporary advances in multi-access edge computing: A survey of fundamentals, architecture, technologies, deployment cases, security, challenges, and directions, Journal of Network and Computer Applications,2023 Volume 219, 103726, https://doi.org/10.1016/j.jnca.2023.103726.
11. T. Ha. A SURVEY ON NOMA WITH THE AID OF INTELLIGENT REFLECTING SURFACE IN WIRELESS COMMUNICATION. International Journal of Research - GRANTHAALAYAH. 2024. 12. 10.29121/granthaalayah. v12.i7.2024.5718.
12. Z. Liu and L. L. Yang. Sparse or Dense: A Comparative Study of Code-Domain NOMA Systems. 2020. arXiv:2009.04148v1
13. V. Vikas, K. Deka, S. Sharma and A. Rajesh, "ADMM-Based Detector for Large-Scale MIMO Dense Code-Domain NOMA Systems," in IEEE Transactions on Vehicular Technology, vol. 73, no. 11, pp. 17024-17040, Nov. 2024, doi: 10.1109/TVT.2024.3424690.
14. G. Sanjeev. Non-Orthogonal Multiple Access. Advance computing and Communication. 2019, 3(2). https://journal.accsindia.org/show.article.php?id=42
15. Sony, D. and Keerthi, P. and Aditya, O. and Sravya, N., Simulation and Performance Analysis of Interleave Division Multiple Access (IDMA) in Comparision with Code Division Multiple

Access (CDMA) (2021). Asian Journal of Applied Science and Technology (AJAST), Volume 5, Issue 2, Pages 90-94, April-June 2021, Available at SSRN: https://ssrn.com/abstract=3874604.

16. I., Budhiraja, N. Kumar, S. Tyagi, S. Tanwar, Z. HAN, M. D. J. Piran and D. Y. Suh. A Systematic Review on NOMA Variants for 5G and Beyond. IEEE ACCESS. 2021. 10.1109/ACCESS.2021.3081601.
17. T. V. Tai, M. P. Nhut Tan, L. H. Nam, N. V. Ha and T. T. Thao Nguyen, "Convergence Evaluation of OFDMA-IDMA Combination Based on IEEE 802.11ax," 2024 16th International Conference on Knowledge and Smart Technology (KST), Krabi, Thailand, 2024, pp. 248-253, doi: 10.1109/KST61284.2024.10499693.
18. H. Marne, and P. Mukherji. Performance Enhancement of Bit Error Rate with Increased Capacity using Modified SIC-MUD for Polar Code based OFDM-IDMA System for 5G. International Journal of Innovative Technology and Exploring Engineering (IJITEE), 2019, 8(9S3): 192-200.
19. P. Agarwal and M. K. Shukla . MITA interleaver for OFDM-IDMA and SCFDMA-IDMA techniques using QPSK modulation over PLC. Bulletin of Electrical Engineering and Informatics. 2022. 11(3): 1418– 1427.
20. M. Jadhav, V. Deshpande, D. Midhunchakkaravarthy, and D. Waghole. Improving 5G network performance for OFDM-IDMA system resource management optimization using bio-inspired algorithm with RSM, Computer Communications, 2022, Volume 193, Pp. 23-37, https://doi.org/10.1016/j.comcom.2022.06.031.
21. M. Kawata, K. Tateishi, and K. Higuchi. Performance Evaluation of IDMA-Based Random Access with Various Structures of Interference Canceller. IEICE Transactions on Communications. 2020, E103. B. 10.1587/transcom.2019EBP3220.
22. D. Dinesh, S. Devadoss and R, Shantha. Fully parallel low-density parity-check code-based polar decoder architecture for 5G wireless communications. Etri Journal. 2023, 46. 10.4218/etrij.2023-0002.
23. J. Zhang. Performance Enhancement of IDMA System by Power and LDPC Code Optimization. International Conference on Wireless Communication, Network and Multimedia Engineering (WCNME 2019) 2019. 10.2991/wcnme-19.2019.25.
24. M. A. S. Al-Adwani, and H. Hamdoon. Simulation and Performance Evaluation of Non-Orthogonal IDMA for Future Wireless Networks. Journal of Engineering Science and Technology, 2019, 14(4): 1835 – 1850.
25. A. Bala, J. D. Jiya, E. E. Omizegba, S. Y. Musa, M. B. Aminu, and H. M. Sabo. Multi-Objective Optimization Power Control for DS-CDMA Using Bacterial Foraging Algorithm. International Journal of Engineering, Technology, Creativity and Innovation. 2019, 2(3): 1-21.
26. M. A. Charar, and Z. Guennoun. Energy Efficient Power Control for Device to Device Communication in 5G Networks. International Journal of Electrical and Computer Engineering (IJECE). 2020, 10(4), 4118 - 4135.
27. X. Wang, Z. Wang and Q. Liang. Outage Throughput Capacity of Hybrid Wireless Networks Over Fading Channels. IEEE Access: Special Section on New Waveform Design and Air-Interface for Future Heterogeneous Network towards 5G, 8 2020: 867-875.
28. S. Bajpai and D. K. Srivastava (2015). Comparative Analysis of OFDM IDMA Scheme by Varying the Users. International Journal for Scientific

Research & Development (IJSRD), 3(1): 1067 - 1069.
29. I. K. Abboud, F. A. Muaayed , and A. A. Nasir. Performance Analysis of Interleave Division Multiple Access System. International Journal of Open Information Technologies. 2019, 7(6). file:///C:/Users/Hp/Downloads/performance-analysis-of-interleave-division-multiple-access-system%20(1).pdf
30. Hu, Y., Ping, L. (2019). Interleave Division Multiple Access (IDMA). In: Vaezi, M., Ding, Z., Poor, H. (eds) Multiple Access Techniques for 5G Wireless Networks and Beyond. Springer, Cham. https://doi.org/10.1007/978-3-319-92090-0_13
31. S. Dixit, V. Shukla, and M. K. Shukla. Progressive Pattern Orthogonal Interleaver Set for Interleave Division Multiple Access Based, Non-Orthogonal Multiple Access Schemes: Beyond 5G Perspective. International Journal of Electrical Engineering, 2022, 73(6): 419 - 425.
32. Wang Z, A Q, Zhu Z, Fang H, Huang Z. Blind Additive Gaussian White Noise Level Estimation from a Single Image by Employing Chi-Square Distribution. Entropy. 2022; 24(11):1518. https://doi.org/10.3390/e24111518
33. A. J. Rojas, "Nonminimum Phase Zeros Effect on the Signal-to-Noise Ratio Channel Input Constraint in Continuous Time," 2024 American Control Conference (ACC), Toronto, ON, Canada, 2024, pp. 1281-1286, doi: 10.23919/ACC60939.2024.10644579
34. R. Mahmoud and S. Mohamed. New Mathematical Properties for Rayleigh distribution. Jurnal Matematika, Statistika dan Komputasi. 2022, 19. 223-234. 10.20956/j. v19i1.21946.